

## Anisotropic surface tension for adaptive self-folding processes

### Applicants

Pierre Lorenz, Dr. rer. nat.

Nationality: German

Private: Möckernschestraße 28, 04155 Leipzig

Employee: Leibniz –Institute of Surface Engineering (IOM), Permoserstraße 15, 04318 Leipzig

Phone: +49 341 235 – 3291

Mobile: +49 176 217 280 82

E-mail: [pierre.lorenz@iom-leipzig.de](mailto:pierre.lorenz@iom-leipzig.de)

Abbreviation: IOM

### Cooperating institution / partner

Gregory Lecrivain, Dr. rer. nat.

Helmholtz-Zentrum Dresden-Rossendorf

Institut für Fluidodynamik

Bautzner Landstraße 400, 01328 Dresden

Phone: +49 351 260 – 3768

E-mail: [g.lecrivain@hzdr.de](mailto:g.lecrivain@hzdr.de)

Abbreviation: HZDR

*The cooperation planned in the scope of the SPP 2171. The funds will be requested by Dr. G. Lecrivain in the SPP project “Direct numerical simulation of droplet impact with a deformation fluidic substrate”.*

## Project Description

### 1 State of the art and preliminary work

#### 1.1 State of the art

The project will affect a variety of different scientific and technological aspects, such as liquid-solid state interaction (contact angle, 3D self-folding processes), fabrication of micro- and nanostructures on surfaces, or structuring of flexible substrates. The scientific and technological status of the various aspects will be discussed briefly below.

##### 1.1.1 Contact angle

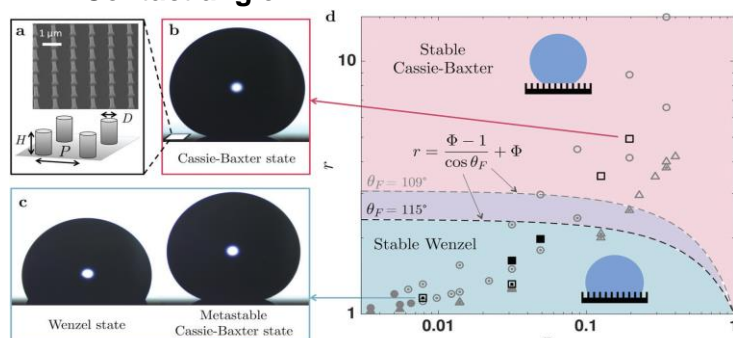


Figure 1: (a) SEM image and a schematic illustration of the hydrophobic nanostructures and the resulting wetting (Cassie-Baxter state) (b) wetting at Wenzel state and metastable Cassie-Baxter state (c) Formation of stable Wenzel and Cassie-Baxter states depending on the geometry of the nanostructures: surface roughness

$r = 1 + (\pi \cdot D \cdot H)/P$  and ratio of the surface involved  $\phi = (\pi \cdot D^2)/(4 \cdot P^2)$  [5]

The interaction of liquids with a solid surface in a gas atmosphere is a centuries-old problem. In 1805, Thomas Young published the Young's equation [1]:

$$\gamma_{SG} = \gamma_{SL} + \gamma_{LG} \cdot \cos\theta \quad (1)$$

with  $\gamma$ : interfacial tension (SG: solid/gas interface, SL: solid/liquid interface, LG: liquid/gas interface) and  $\theta$ : contact angle. It is known that chemical and morphological surface modifications can significantly affect the contact angle, like hydrophilic ( $\theta \approx 0^\circ$ ) in water, hydrophobic ( $\theta \approx 90^\circ$ ) to superhydrophobic ( $\theta \approx 160^\circ$ ). In recent

years, the technological development in the micro- and nanostructuring processing has led to an increased scientific interest in the field of influencing contact angles by surface structures [2]. The influence of the contact angle by surface structures has been known for almost 100 years. R.N. Wenzel reported that a fine structure changes the contact angle  $\theta_w$  [3]:

$$\cos\theta_w = r \cdot \cos\theta \quad (2)$$

where  $r$  is the ratio of the actual area to the projected area, with the assumption that the liquid wets the entire fine structure. According to Cassie and Baxter [4], a partial wetting of the fine structure results in a modified contact angle  $\theta_{CB}$ :

$$\cos\theta_{CB} = \phi \cdot [\cos\theta + 1] - 1 \quad (3)$$

with  $\theta$ : contact surface between solid and liquid and under the condition  $\cos\theta < (\phi-1)/(r-\phi)$ . Advanced models, i.e., Extrand et al. [6], allow a prediction of the behavior as a function of the structural parameters, such as the contact line density  $p$ . The critical contact line density can be described by:

$$\Lambda_c = \frac{-\rho \cdot g \cdot V^{1/3} \left( \left( \frac{1-\cos\theta_a}{\sin\theta_a} \right) \left( 3 + \left( \frac{1-\cos\theta_a}{\sin\theta_a} \right)^2 \right) \right)^{2/3}}{(36\pi)^{1/3} \cdot \gamma \cdot \cos(\theta_{a,0} + w - 90)} \quad (4)$$

with  $\theta$ : density of the liquid,  $g$ : gravitation constant,  $V$ : volume of the liquid,  $\theta_a$ : last contact angle before a movement,  $\theta_{a,0}$ : last contact angle before moving on a smooth surface,  $\gamma$ : surface tension of the liquid and  $w$ : tower wall angle. The condition  $\Lambda > \Lambda_c$  describes a Cassie-Baxter state and  $\Lambda < \Lambda_c$  describes a Wenzel state. Furthermore, the structured surfaces allow the fabrication of anisotropic contact angle e.g. by periodic structured photoresist [2]. The fabrication of anisotropic contact angle by the interaction of a liquid droplet with a structured surface can be simulated by finite element method (FEM) [7].

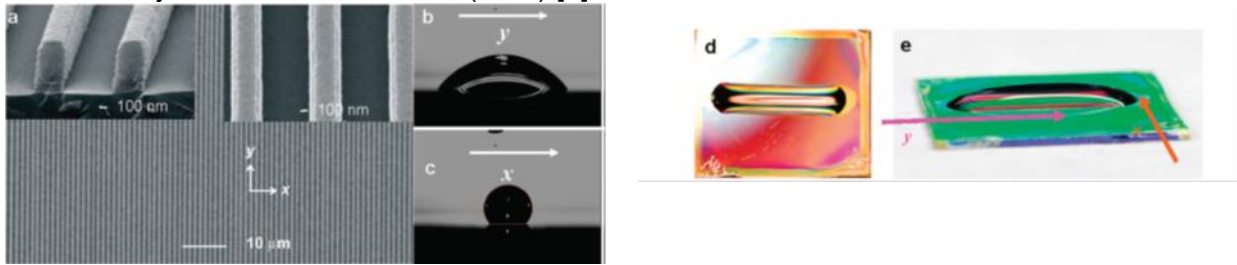


Figure 2: 1D, 1500 nm period photoresist (PR) structures and the anisotropic wetting: (a) Large area SEM image; (b) contact angle  $\theta_y$ , parallel to the direction of the lines; (c) contact angle  $\theta_x$ , orthogonal to direction of lines; (d) and (e) photograph of top view and side view of the droplet, respectively [2].

➔ **Conclusion: Micro- and nanostructures can induced an anisotropic wetting angle.**

### 1.1.2 Micro- and Nanostructuring of flexible substrates

In the recent years continuous development, in particular in communication technologies, has steadily advanced the development in the processing of flexible substrates. This trend is reinforced by the development of mass products in the fields of lighting (organic light emitting diode (OLED)), photovoltaic, transponder technology, and the electronic newspaper. Examples for technologies for surface micro- and nanostructuring are summaries below [29]: - Interference lithography, nanoimprint lithography, block copolymer self-assembly, wrinkling, inclined lithography, multi-photon lithography, replica moulding, MACE: metal-assisted chemical etching, GLAD: glancing-angle deposition, OAP: oblique angle polymerization, oriented nanostructure growth, elastocapillary self-assembly, directed mechanical deformation. The flexibility requirements of the flexible substrates may include rollability, stretchability, or general deformability, depending on the application. Important flexible substrates include metal tapes, plastic films, or fiber-reinforced composites. Taking into account economic and functional aspects, polymeric films have a preferred position as a substrate material due to high flexibility, good surface finish, technical availability, low manufacturing cost, roll-to-roll processability, etc. Important polymers for flexible substrates are the thermoplastics, e.g. polyethylene terephthalate (PET) and polycarbonate (PC) and the thermosets, e.g. polyimide (PI) and polyacrylate (e.g., PAR). The high chemical stability of these materials make wet-chemical structuring processes almost impossible. Dry chemical etching processes require a multi-step processing including e.g. masking (metal mask) and vacuum process. Laser ablation, on the other hand, has great potential for structuring flexible substrates and flexible functional layers. For the laser structuring of flexible

substrates, a variety of methods are known. Selected additive and subtractive laser-based processes summarized in the following:

- Laser ablation (LA): Explosive physically dominated material removal with pulsed lasers.
- Laser etching (LE): Laser-induced chemical reactions with the dissolution of the target material.
- Laser backside etching (LIBWE): Physical removal of a laser-modified material.
- Laser CVD (LCVD): Local deposition of material by chemical reactions.
- Laser-induced layer transfer (LIFT): Transfer of layer (packages) from a donator surface to the target substrate.
- Laser microsintern ( $\mu$ Sin): Production of (3D) structures by laser sintering of  $\mu\text{m}$  /  $\text{nm}$ -powders.
- Two-photon polymerization (2PP): Localized polymerization of liquid polymers.

Laser-based methods are suitable for the flexible and fast fabrication of polymer-based structures for droplet induced self-folding processes. The optimal use of different laser techniques, including laser ablation, requires the understanding of the laser - solid-state interaction. This needs the specific selection of parameters depending on the material, the specific layer structure, the required geometry of the structure and the tolerable side effects. A wide variety of simple surface topographies can be generated in various materials [8] by subtractive laser methods. The production of 3D microstructures by subtractive on methods requires sophisticated methodological and procedural approaches in contrast to the two-photon polymerization [9-12]. An overview of the possible methods of producing 3D structures by laser ablation is given in Ref. [13]. Further developments of the laser methods will allow the production of more complex topographies by the pre-calculation of laser beam modifying masks and of the laser beam path on the sample surface [14-17].

→ **Conclusion: Polymer substrate surfaces modified and structured by laser methods in micro- and nanometer range as well as the substrate cut in different geometries.**

### 1.1.3 Origami / kirigami structure

The transition of a variety of different plane 2D geometries into 3D structures with defined geometries is a century old issue i.a. in the Japanese culture.

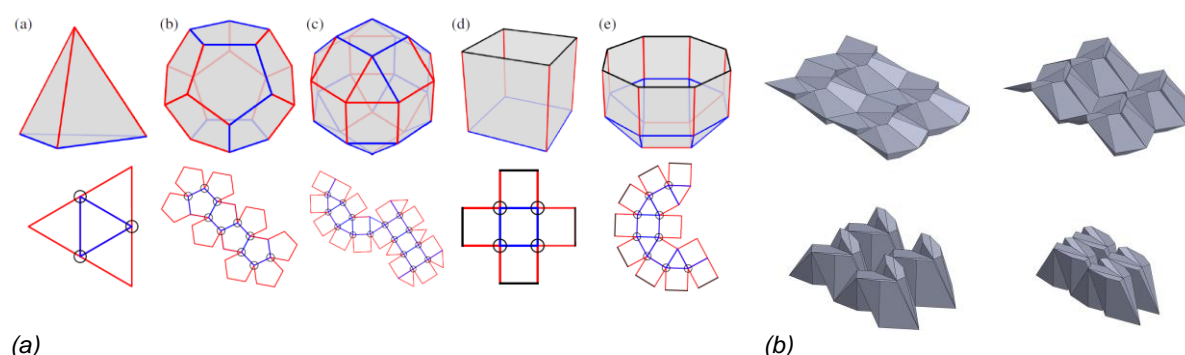


Figure 3: (a) Five examples of shells and a possible net, respectively [18]  
(b) Tapered panels technique applied to the Miura-ori pattern [19]

The terminology origami and kirigami comes from the Japanese language. Origami (*ori*: "folding", *kami*: "paper") is the Japanese art of paper folding where the goal is to transform a flat square sheet of paper into a finished sculpture through folding and sculpting techniques. Kirigami is a variation of origami that includes cutting of the paper. In the last year, the origami concept was adopted in a wide range of technical fields from macro-systems like air bags, robots and space application as well as microsystems like MEMS, electric devices, DNA, and cell origami [19-23]. The suitable plane 2D structures for self-folding 3D structures can be calculated [18], see Figure 3. Besides, simple 2D plane structures the usage of complex structures like Miura-ori pattern [19] (see Figure 3) allows the fabrication of complex folding structures.

→ **Conclusion: 3D structures can be generated from 2D structures by folding processes.**

### 1.1.4 3D self-folding structures

Folding for 3D structures in the millimeter and micrometer range are preferred generated by self-folding processes whereat different physical effects can be used.

#### i. with liquid droplets

The self-folding process induced by a liquid-solid-interaction and a droplet on the plane surface, respectively [24–26]. The droplet can be directly add-on the solid surface [24, 26] (see Figure 4 (a) and (c)) and the liquid can be deliver through the sample surface [25] (see Figure 4c), respectively. In agreement with the theoretical prediction (see Figure 3a), the resultant 3D structures is direct dependent on the original 2D plane structure (see Figure 4 c).

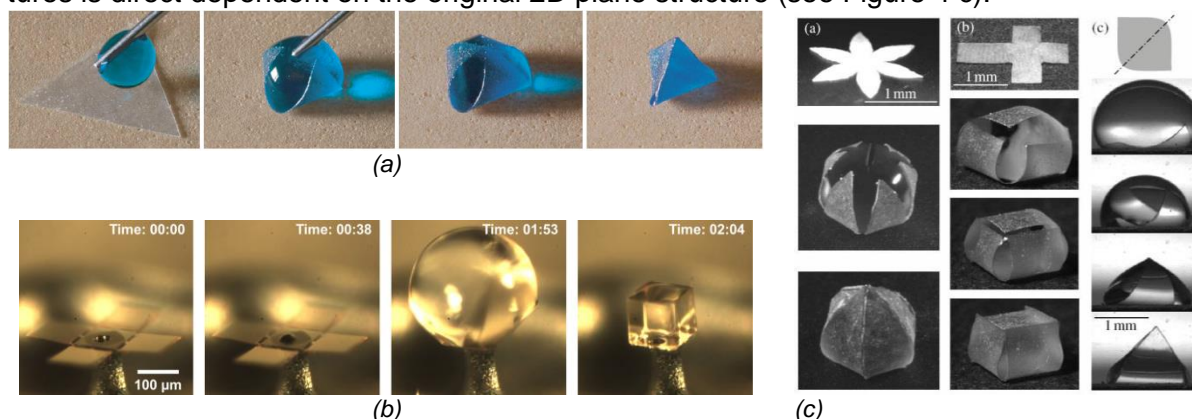


Figure 4: (a) Wrapping of a drop of water with a triangular PDMS sheet, resulting in a pyramid structure [26]. (b) Chronological sequence of images (from left to right: Time: 00:00: cube template, 00:38: liquid application, 01:53: folding, 02:04: folded cube filled) from a video of the folding process of a five-faced SiN cube with a rib length of 100 μm (time format: mm:ss) [25].

(c) Microscopic images of 3D self-folding structures induced by water droplets on pre-structured PDMS films [24]

#### ii. temperature and electric field controllable

The self-folding structure can be controlled by external parameter like temperature and electric field. For example, the usage of multilayer structured thin layer based on thermoresponsive polymers [27] allows the reversible and temperature controllable self-folding, see Figure 5 (a).

Furthermore, the droplet – induced self-folding process can be controlled by an additional electric field, see Figure 5 (b) [28]. The interaction of salty water droplet with an additional electric field allows the direct control of the droplet-induced self-folding process.

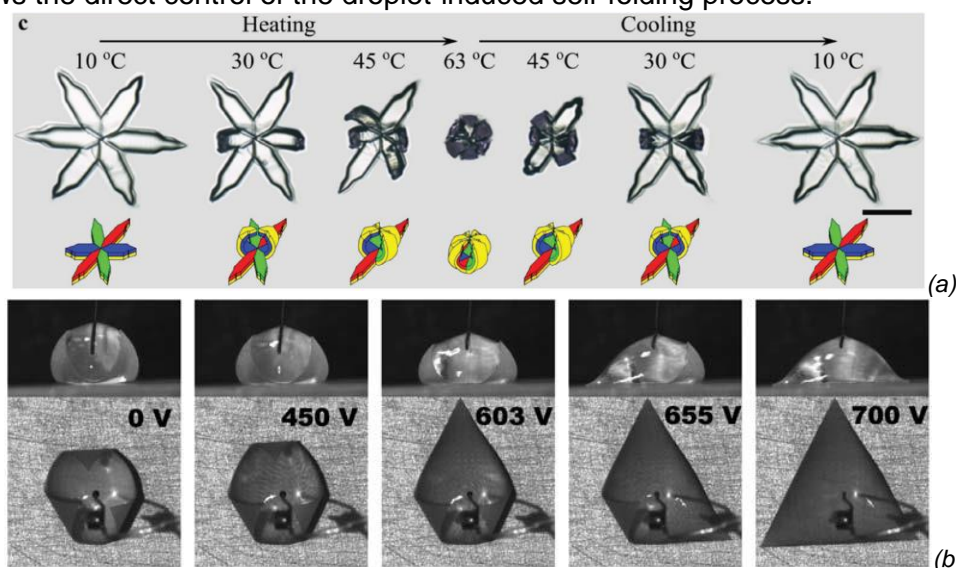


Figure 5: (a) Optical images and schematic representations of four-state shape changes of grippers based on OEGMA<sub>300/500</sub> (poly (ethylene glycol) methyl ether methacrylate  $M_n = 300 / 500$ ) and DEGMA (diethylene glycol methyl ether methacrylate) thin layer stacks and during heating and cooling. The images from left to right are at 10 °C, 30 °C, 45 °C, 63 °C, 45 °C, 30 °C, and 10 °C. Scale bars represent 2 mm [27].

(b) Images of the lateral and upper views obtained during the experiments PDMS sheet with salty water droplet at increasing voltage [28]

→ **Conclusion: Self-folding processes induced by a liquid–solid interaction (liquid droplet) and controlled by external effects (e.g. temperature, electric field).**



### 1.1.5 Preliminary work

At the IOM Leipzig, beam methods (including ion, electron, and laser beam) have been used for surface modification, layer deposition and microstructuring since the foundation. The institute performs application-oriented basic research. The objective of the work of the institute is the fabrication of functional surfaces and layers due to the precision modification of surface topographies and compositions. The existing technologies and experiences of the institute within the framework of this project are synergistically linked.

The applicant and the members of the working group “Laser micro- and nanostructures” have been working in the field of structuring of solid surfaces in recent years using:

- Laser [E2, E3]
- UV lithography and electron beam lithography [E3 – E5]
- (Reactive) ion beam etching ((R) IBE) [E4, E5]
- Sputtering (sputtering) [E5]

Some selected examples discussed in more detail below:

#### - Generation of undercut 3D structures using RIBE [E4]

The directional RIBE treatment of quartz glass covered with a structured chromium layer (structured by UV lithography and wet chemical etching) allows the generation of undercut 3D structures in  $\text{SiO}_2$  (see Fig. 6). Further information can be found in [E4]. Among other things, the undercut structures used in microcompounds [E1].

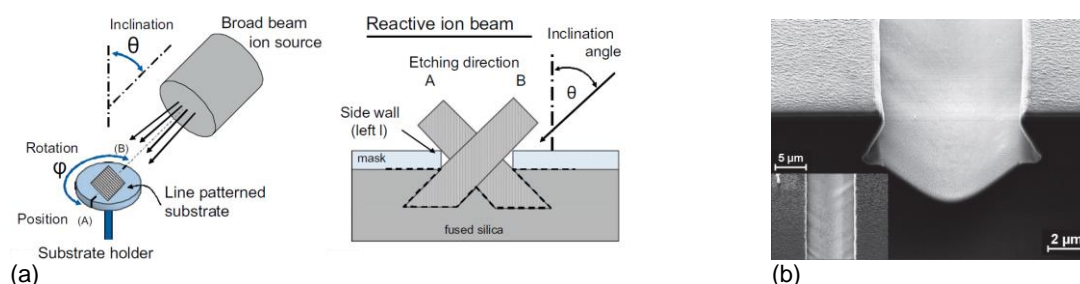


Figure 6: (a) Schematic illustration of the experimental setup for etching of patterns undercut structures: (left) Arrangement of the ion source and the sample holder and (right) view of the cross section with the angle of incidence of the ion beam  $\theta$ . This allows etching from opposite directions by sample rotation of  $180^\circ$ . (b) SEM image of RIBE generated structure in quartz glass [E4].

Furthermore, the coupling of electron beam lithography with sputtering and RIBE allows the fabrication of nanostructures with high aspect ratios [E5]. For this, thermally oxidized silicon sputtered with a thin metal layer and covered with a photoresist. The photoresist patterned by means of electron beam lithography and sputtered subsequently with argon, resulting in a selective structuring of the chromium layer. The RIBE treatment of the sample with a structured chromium layer allows the fabrication of deep structures in  $\text{SiO}_2$  due to the high etch selectivity between Cr and  $\text{SiO}_2$ . Figure 7 shows exemplary  $\text{SiO}_2$  structures.

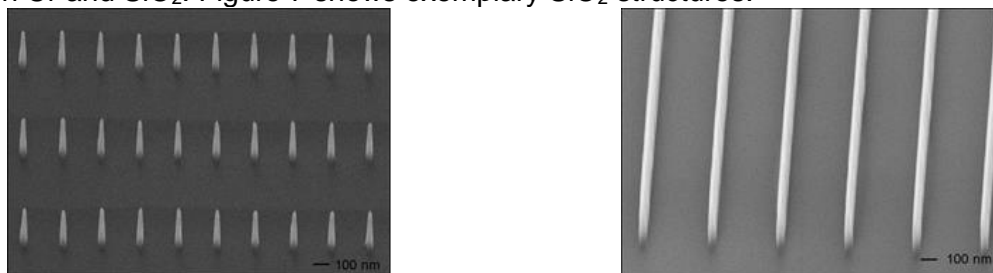
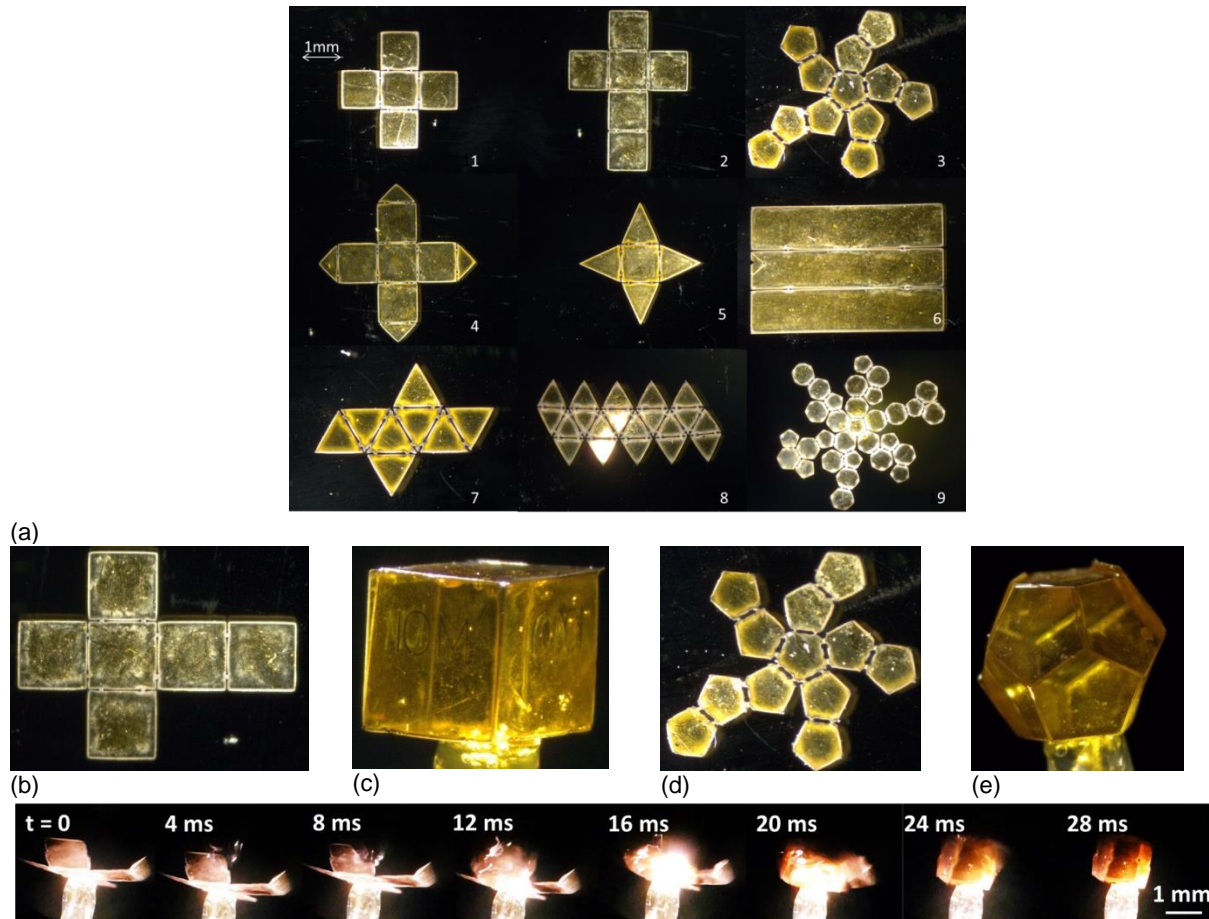


Figure 7: SEM images of prepared  $\text{SiO}_2$  nanostructures with high aspect ratios [E5].

➔ **Conclusion:** The available technologies at the IOM in the field of lithography and plasma and ion beam structuring, and, in particular, the know-how of the employees over decades, allows a synergetic combination of the individual technologies and thus the production of innovative micro- and nanostructures.

### - Laser structuring of flexible and substrates and 3D origami structures

The IOM has many years of experience in the field of laser-assisted structuring of dielectrics, organic, and inorganic semiconductors, metals, and polymers. In Figure 8, microscopic images of exemplary polyimide film (PI) structures prepared by 780 nm fs laser radiation. The delivering of water droplets of suitable volume onto the structured PI surface leads to self-folding of the structured PI film.



(f) Figure 8: Laser-structured PI films (a) (structure line width 50  $\mu\text{m}$ , structure edge length 0.5-1 mm) (b) and (d) structured PI foil as well as (c) and (e) water droplet-induced self-folding 3D structures based on laser-structured PI films (see (a) and (c)) (f) time dependent optical characterization of the self-folding process

➔ **Conclusion: The available laser systems and the existing experience and knowledge enable effective laser-based structuring and modification of flexible substrates.**

### - Laser induced dewetting: experiment and theory [E2, E3]

The laser irradiation of a thin metal layer on a dielectric surface result in melting of the thin layer, whereby the following dewetting process leads to the formation of metal micro- and nanostructures. When using pulsed laser radiation, e.g., nanosecond laser pulses, the lifetime of the melt phase is less than the dewetting time. The dewetting process can be frozen in intermediate states, e.g., with thin metal layers on dielectrics. Melt-phase lifetime and melt-phase velocity can be determined by time-resolved reflection and transmission measurements [E2]. In initial homogeneous and laterally large layers, the dewetting process leads to statistically distributed structures, while the irradiation of laterally small structures leads to deterministic structures (see Fig. 9) [E2, E3]. The temporal dewetting behavior and the resulting structures can be described by the coupling of the heat equation (description laser-solid-state interaction including phase transformation) and the Navier-Stokes equation (description of the mass transport in the melt phase). The coupling takes place via the temperature-dependent material parameters.

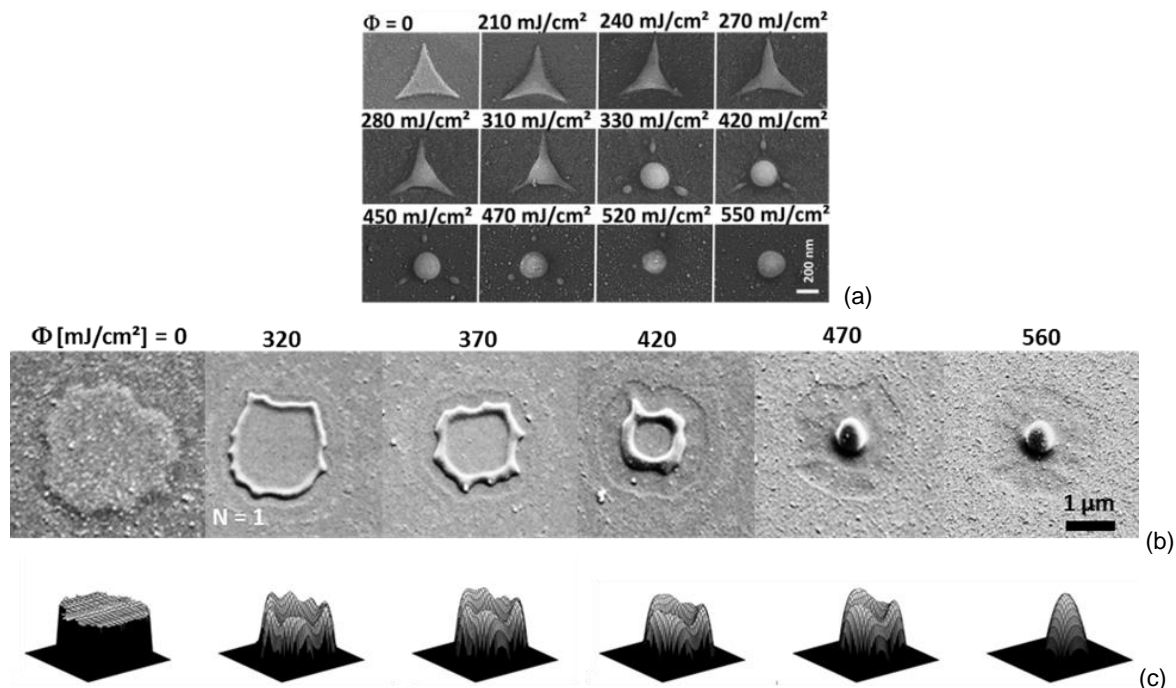


Figure 9: (a) SEM images of 30 nm thick Cr triangles on SiO<sub>2</sub> irradiated by a single laser pulses with different laser fluences [30]. (b) SEM images of photolithographically structured 7 nm high chromium structures irradiated with KrF excimer laser single pulses with different fluences [E3]. (c) Simulation of the dewetting process of chromium structures at different time steps and corresponds laser fluences.

## 1.2 Project-related publications

### PDMS

[E1] Measurement and simulation of the pull-off strength at the separation of miniaturized 3D connectors consisting of silicon masters with undercuts and PDMS replicas,  
J. Zajadacz, P. Lorenz, M. Ehrhardt, K. Zimmer, S. Möllenbeck, K. Dhima, H.C. Scheer,  
Microelectronic Engineering 101 (2013) 31-36

### Dewetting

[E2] Dynamics of the laser-induced nanostructuring of thin metal layers: experiment and theory  
P. Lorenz, M. Klöppel, T. Smausz, T. Csizmadia, M. Ehrhardt, K. Zimmer, B. Hopp  
Materials Research Express 2 (2015) 026501

[E3] From statistic to deterministic nanostructures in fused silica induced by nanosecond laser radiation  
P. Lorenz, M. Klöppel, I. Zagoranskiy, K. Zimmer  
Procedia CIRP 74 (2018) 371–375

### Micro- / Nanostructuring

[E4] Fabrication of optimized 3D microstructures with undercuts in fused silica for replication  
K. Zimmer, J. Zajadacz, R. Fechner, K. Dhima, H.C. Scheer,  
Microelectronic Engineering 98 (2012) 163-166

[E5] Fabrication of high aspect ratio sub-100 nm patterns in fused silica  
J. Zajadacz, R. Fechner, K. Zimmer,  
Journal of Materials Science and Engineering A 2 (2012) 458-462

## 2 Objectives and work program

### 2.1 Anticipated total duration of the project

The project is designed for 3 years and the funds are requested here.

### 2.2 Objectives

The final aim of the project is the production of 3D self-folding structures based on structured thin polymer films with adjustable surface and volume properties. To order to achieve this aim, different scientific questions must be investigate. The general theses of the project are:

*The liquid-solid-surface interaction (L-S-I), in particular, dewetting phenomena, can be influenced by chemical and topographical modification. Furthermore, the L-S-I leads to an additional force on the substrate surface, which can result in a self-folding 3D structures using a suitable substrate structure.*

The aim of the project is the production of self-folding structures under the assumption of the following theses and the questions derived from them. In order to achieve the aim of the project, different technological, experimental and theoretical aspects need to take into account. In the following, the different *thesis* and derived questions are structured and presented according to the different aspects.

#### - Anisotropic contact angle and L-S-I

*Thesis: The contact angle can be influenced by chemical and topographical modifications.*

- Which substrate surfaces are suitable for the reproducible setting of a contact angle, in particular, under the objective of producing anisotropic contact angles?
- In which range can an anisotropic contact angle be generated?
- How does the contact angle can be change depending on external influences, such as temperature, pressure or gas composition?

*The anisotropic contact angle can be achieved and adjusted by determined modification of the substrate surface.*

- In which ranges (direction-dependent variation of the contact angle) is an anisotropic contact angle able to be changed by modification of the substrate surface i.e., by stretching?
- In which range can the contact angle reversible varied by the reversible variation of the substrate surface properties?

*The L-S-I results in a force on the substrate surface.*

- How large is the L-S-I induced force on the substrate as a function of the modification of the substrate surface and external influences (temperature, pressure, or gas composition)?

#### - Anisotropic mechanical properties

*An adjustable modification of a substrate, e.g., composition of polymers with different elastic modulus or sieve structures allows a systematic anisotropic adjustment of mechanical properties.*

- Which geometries and material combinations are suitable for the reproducible production of substrates with anisotropic mechanical properties?
- Which mechanical parameters, such as elastic modulus and poisson number can be generated depending on the selected geometries and material properties?
- Are the modified substrates long-time stable? Are there any changes in the effective mechanical characteristics with periodic measurement of force-strain curves?

#### - 3D self-folding processes

*The L-S-I-induced forces allow the formation of 3D self-folding structures when used with suitable substrate geometries.*



- Which substrate geometries, including the "hinge-joint" geometries (bend areas during the folding process), are suitable for forming 3D self-folding structures?
- Is the 3D self-folding process scalable? (The intended production technologies determine the range of producible structure sizes of the 3D self-folding structures from ~ 1  $\mu\text{m}$  to several 10 cm.)

*The use of substrate and surface modifications, particularly those which produce lateral variable and anisotropic contact angles, and mechanical substrate properties, allow direct manipulation of the 3D self-folding process.*

- How can the dynamics of the 3D self-folding process influence by surface modifications?
- Which resulting 3D structures achieved dependent on surface modification?
- How does substrate modification affect the dynamics of the 3D self-folding process?

*The combination of systematic substrate surface and substrate bulk modification allows a direct, reversible, and predictable adjustment on the 3D self-folding process. This allows a significant extension of the achievable geometries of the self-folding process.*

- Which geometries are achievable?
- What are the experimental and theoretical limits of the modified folding process?

#### - Physical description and simulation of the processes

*The influence of the substrate modification on the "macroscopic" mechanical properties described with a linear elastic approach (in some cases a hyperelastic approach) and the mechanical properties can be simulated.*

*The L-S-I described by the mass transport of the liquid phase by the Navier-Stokes equation, whereby the L-S-I is influenced by the surface modification. This can be i.e., described by Wenzel and Cassie-Baxter states.*

*The coupling of the mechanical, physical description with the L-S-I allows a simulation of the 3D self-folding process.*

Based on the theses and the derived questions, the project divided into two phases: PHASE 1: Fundamentals Investigations of the L-S-I. and PHASE 2: Self-folding 3D structures. The planned work packages will be discussed in more detail in the next section.

### **2.3 Work program incl. proposed research methods**

In order to achieve the aim of producing 3D folding structures with adjustable surface and bulk properties, the project divided into two phases (see Fig. 10). The first phase (PHASE I) focuses on the investigation of the L-S-I, and the second phase (PHASE II) on the fabrication of 3D self-folding structures. In PHASE I, the influence of additive and subtractive micro- and nanostructures (WP 1.1 and WP 1.2), as well as chemical modification (WP 1.2), on the L-S-I are investigated. In addition to the surface modification of the flexible substrate, the setting of anisotropic physical quantities (e.g. spatial variation of the modulus of elasticity, heat conduction, initial layer stress) (WP 1.3), allows a significant extension of the resulting structures of the 3D self-folding structures. It is also necessary to expand the understanding of L-S-I depending on external influences, such as temperature, pressure, ambient gas composition, and external tensile forces (WP 1.4). In particular, the contact angle is examined as a function of the substrate modification and the L-S-I-induced force on the substrate. In addition to the L-S-I, the mechanical properties of the substrates produced in WP 1.3 investigated in WP 1.4. For this purpose, a special measuring system will be set up in WP 1.4. To understand the results of WP 1.4, the mechanical properties of the modified substrates (WP 1.5 a) and L-S-I (WP 1.5 b and c) are simulated by finite element method. Based on the results of WP 1.4 and WP 1.5, an optimization of the structures carried out, in particular based on the results and predictions of the simulations. Based on the results of PHASE I, PHASE II focuses on the fabrication of self-folding 3D structures.

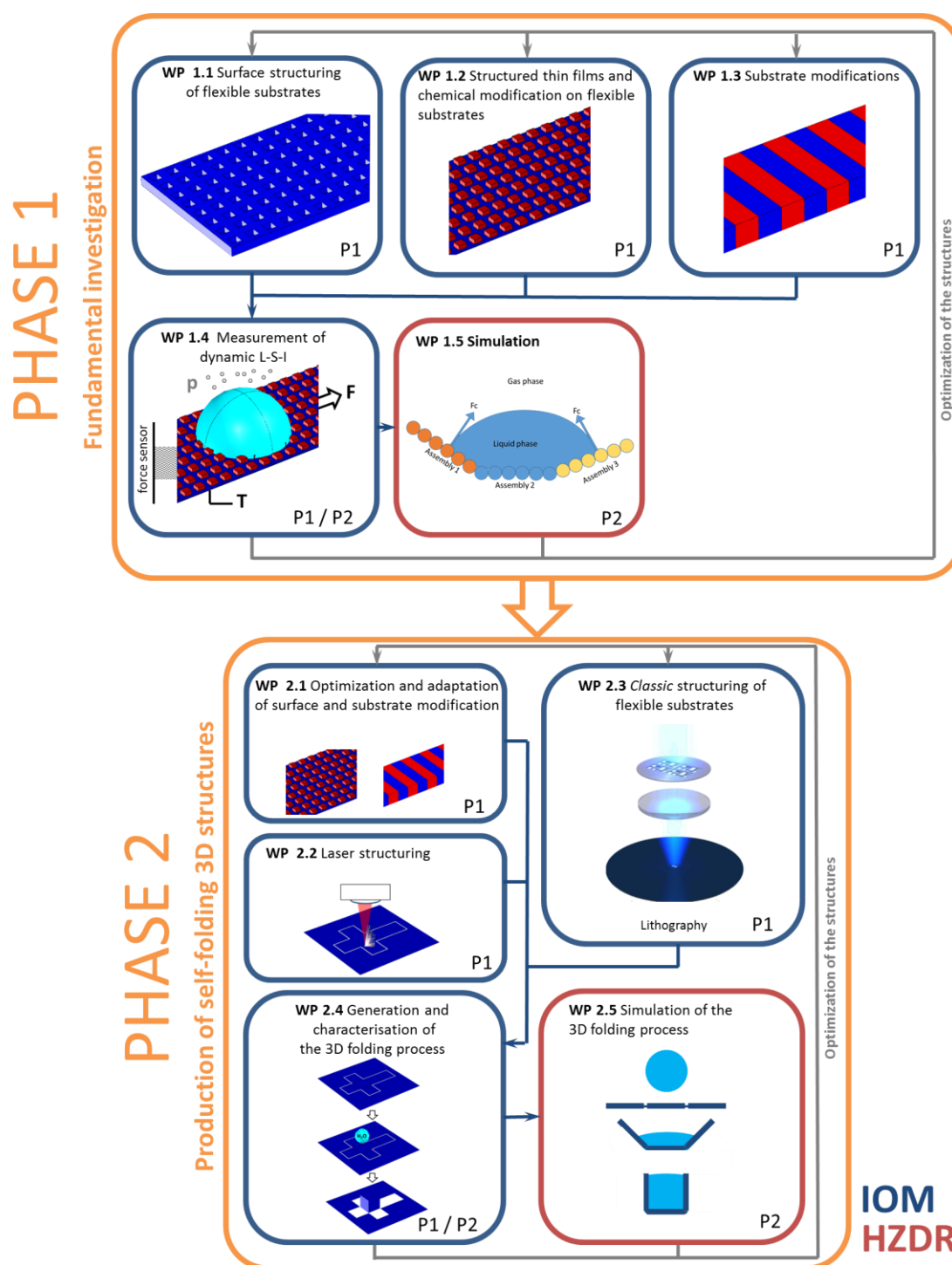


Figure 10: Schematic representation of the work packages (color coded: “blue” edges work package is performed by IOM, “brown” edges work package is supported by HZDR) P1: Work package is performed by PhD student 1 and P2: performed by PhD student 2

For this purpose, suitable substrate and surface modifications selected in the first step and, if necessary, adapted and optimized based on the results from PHASE I (WP 2.1). In the next step, the planned samples structured by laser (WP 2.2) and lithographic technologies (WP 2.3). The direct laser structuring (WP 2.2) enables the rapid and flexible structuring of prototypes and is particularly suitable for optimizing the geometries for self-folding structures. Traditional lithographic technologies, especially UV photolithography, allow the rapid, cost-effective mass production of structures (WP 2.2). The results of WP 2.3 allow for the successful implementation of the project a simple transfer of the results to an industrial application. To understand the folding process, the process is time-resolved, studied using the measurement setup created in WP 1.4

(including a camera with a high frame rate ( $\geq 1000$  fps)). Using the optimized physical description of the L-S-I in WP 1.5, a simulation of the convolution process performed in WP 2.5 compared to the measured process (WP 2.4). Based on the successful simulation of the folding process and the resulting structures, the WP 2.5 allows optimization of the lateral planar base geometry of the flexible substrate as well as the surface structure and substrate modifications. The targeted adjustment of the L-S-I by means of surface and substrate modifications allows the generation of various 3D self-folding structures.

**The coupling of various concepts (substrate and surface modifications as well as external influences) allows a significant extension of the achievable self-folding structures. The aim of the project is the evaluation of theoretically and experimentally achievable 3D structures.**

## **Phase 1: Fundamental investigation**

### **Work package WP 1.1 Surface structuring of flexible substrates**

The aim of the work package is the defined surface structuring of flexible substrates. For this purpose, a wide variety of technology approaches is available and planned at the institute. The substrate material used is polymer-based flexible substrates like polydimethylsiloxane (PDMS), polyimide (PI), polypropylene (PP), and polyethylene (PE). The surfaces of the substrates structured by various methods. Hierarchical structures can be achieved by combination of the different technology concepts by e.g. mix and match patterning.

#### **- Laser structuring**

The laser irradiation of the polymer surface with pulsed laser radiation with wavelengths of 248 nm - 1550 nm and pulse lengths of 150 fs to 600 ns and modulated laser beam profiles (with phase masks or spatial light modulator (SLM)) is used for large-scale generation of periodic structures. Structure sizes from sub-mm to sub- $\mu\text{m}$  with high aspect ratios can be produced.

#### **- Electron beam and UV lithography**

The use of electron beam and UV lithography allows the large-area structuring of surfaces with feature sizes of  $\geq 1 \mu\text{m}$  (UV lithography) and  $\geq 20 \text{ nm}$  (electron beam lithography). For this purpose, the polymer surface is coated with photoresist by spin coating and structured by lithography. The patterned photoresist on the flexible substrate is treated by (R)IBE, sputtering, and plasma treatment. This treatment results in local lateral removing and chemical modifications of the substrate surface.

#### **- Moulding**

In addition to direct structuring, a molding process allows the direct production of flexible substrates with defined surface structures. The process is particularly suitable for PDMS. The required master structures can be produced by means of laser structuring and lithography. The generated structures are analyzed by optical (OM), scanning electron (SEM), and atomic force microscopy (AFM). In addition, possible chemical modifications are analyzed by means of Raman spectroscopy (RS), energy dispersive X-ray spectroscopy (EDX) and X-ray photoelectron spectroscopy (XPS).

### **Work package WP 1.2 Structured thin films and chemical modifications on flexible substrates**

In addition to the subtractive substrate surface modification (WP 1.1), additive surface treatments also allow the influence of the L-S-I. There are different technological approaches available and planned, such as:

- Wet chemical modifications e.g., self-assembled monolayer (SAM): octadecyltrichlorosilane (OTS),
- Plasma treatment:  $\text{O}_2$  – plasma, CF plasma
- Metallic and dielectric layer production by cathode sputtering and evaporation

The additive approaches allow the homogeneous treatment of the surfaces and the lateral variation of the modification on the substrate surface by UV lithography. The resulting surfaces determined by OM, SEM AFM, RS, EDX, and XPS.

### Work package WP 1.3 substrate modifications

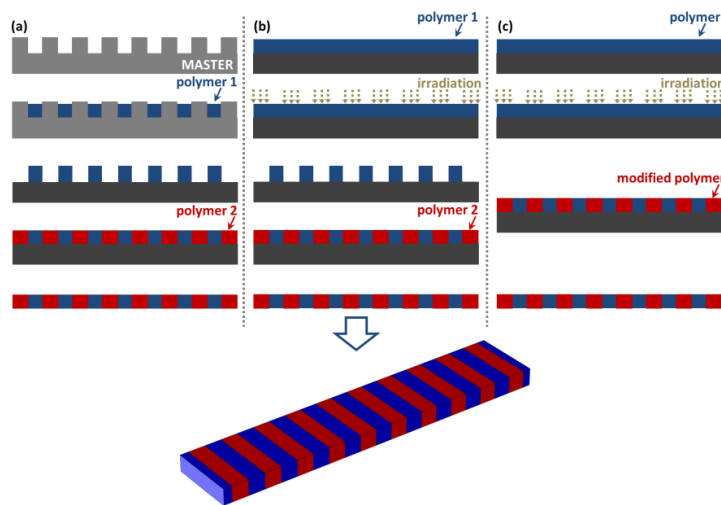


Figure 11: Figure 11: Schematic illustration of the technological approaches to the generation of modified substrates  
 (a) polymer nanoimprint lithography  
 (b) photolithography  
 (c) electron-, ion- and photon beam induced modification of the polymer films

The surface modifications (WP 1.1 and WP 1.2) allow the direct influence of the L-S-I. However, the resulting structure is a combination of the deformation of the substrate and the force generated by L-S-I. The targeted adjustment of the mechanical and thermodynamic properties, e.g., lateral variation of the elastic modulus, allows the generation of an anisotropic elastic modulus. Various technological approaches are used to produce modified substrates; including sieve structures (see Figure 11). The technological approaches used as described in WP 1.1. In addition to producing closed structures based on the combination of different polymers or the selective modification of a polymer, the technological approaches enable the production of sieve structures.

### Work package WP 1.4 Build a measuring system and measurements of the dynamic L-S-I

In order to measure the mechanical properties of the modified substrates (WP 1.3) and the L-S-I of the adapted surfaces (WP 1.1 and 1.2), a measuring system is established. The schematic structure of the measuring system showed in Figure 9, where the structure is based on the appropriate extension of existing measuring systems. To determine the anisotropic properties, the use of a 4-legged sample geometry with modified substrate and surface properties (WP 1.1 - 1.3) is intended, see Figure 12 a. The set-up allows the application of external tensile forces  $F_{\text{trac}}$  from two spatial directions and the measurement of the directional tension. In addition, the design allows the determination of the L-S-I generated stress in the substrate during the application of droplets. These experiments can be performed at adjustable environmental conditions, such as temperature  $T$ , pressure  $p$ , and ambient gas composition. In addition to the mechanical characterization, the measuring system allows an optical analysis of the contact angle, see Figure 12 b, depending on  $F_{\text{trac}}$ ,  $T$ ,  $p$ . Due to the periodic variation of  $F_{\text{trac}}$ ,  $p$  and  $T$ , the measuring station allows a dynamic and reversible variation of the contact angle (see Fig. 12 c). This measurement methodology allows an estimate of the long-time stability of the applied surface modifications.



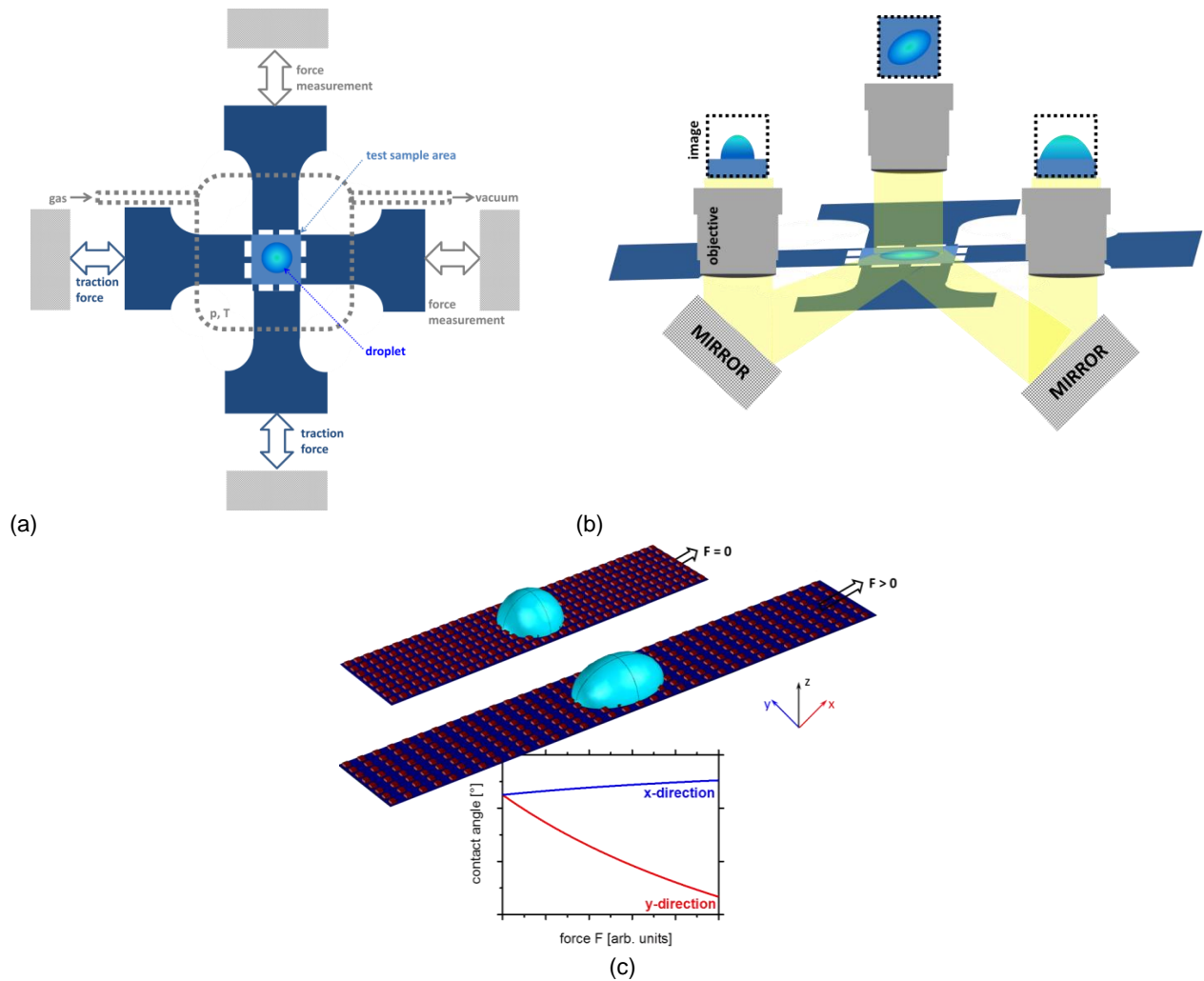


Figure 12: Schematic illustration of the measuring system

(a) Front view of the measuring system with the schematic illustration of the mechanical manipulation and measurement of the sample at adjustable temperatures, pressure, and gas composition

(b) Side view of the measuring system with the schematic illustration of the optical measurement setup for the dynamic determination of the anisotropic contact angle

(c) Schematic representation of reversible dynamic anisotropic contact angles induced by surface modifications on flexible substrates

The WP 1.4 divided into different sub-work packages:

(a) Build-up of the measuring system

(b) Measurements of mechanical effects

b.1. Direction-dependent force-strain curves of modified substrates, depending on the temperature

b.2 Measurement of the directional forces generated by the L-S-I surface and substrate modified samples

b.3 Long-term test: Periodic variation of external factors ( $p$ ,  $T$ ,  $F_{\text{trac}}$ ) for testing the stability of the substrates and surface modifications

(c) Optical measurement of the contact angle

c.1 Determination of the anisotropic contact angle for surface-modified samples

c.2 Dynamic determination of the anisotropic contact angle with adjustable external factors ( $p$ ,  $T$ ,  $F_{\text{trac}}$ )

c.3 Long-time test: periodic variation of the influencing variables ( $p$ ,  $T$ ,  $F_{\text{trac}}$ ) for determination of the stability of the surface modification

## Work package WP 1.5 Simulation (supported by HZDR)

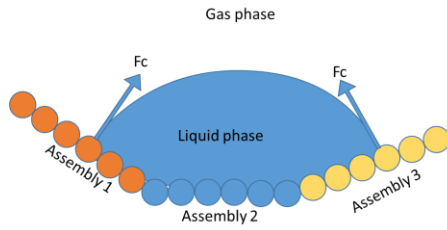


Figure 13 Schematic illustration of the liquid droplet

To improve the physical understanding of the measurements made in WP 1.4 and derive optimizations of the surface and substrate modifications, a physical description of the processes is necessary. The simulation of the liquid droplet – solid film interaction is supported by HZDR. The thin surface of the origami structure is decomposed into a collage of flexible bead assemblies. As illustrated in Figure 1, each assembly is itself geometrically decomposed into a plate of spherical beads bonded between themselves. Each bead of an assembly under-

goes stretching, bending, and torsional deformation. The stretching force, acting on the  $i$ -th bead of the chain, will be modelled as

$$\mathbf{F}_i^s = -k_s(|\mathbf{X}_{i+1} - \mathbf{X}_i| - 2r_b) \mathbf{t}_i,$$

where  $k_s$  was the stretching modulus,  $\mathbf{X}_i$  the position of the  $i$ -th bead,  $r_b$  the particle bead radius, and  $\mathbf{t}_i = (\mathbf{X}_{i+1} - \mathbf{X}_i)/|\mathbf{X}_{i+1} - \mathbf{X}_i|$  a unit vector describing the local bond direction. The bending and the torsion will be implemented in a similar fashion. In order to enable the folding to occur, a rotation allowed at the bond holding the two assemblies. The three dimensional hydrodynamic/capillary simulation is performed using the Extending Smooth Profile Method [31], developed by G. Lecrivain. In this method, each bead sharp boundary of the sphere is replaced with a diffuse interface, across which its volume fraction  $\phi_b(\mathbf{x}, t)$  undergo a smooth but rapid transition from unity to zero as one moves from the inner bead region to the outer bead region. For the binary fluid, a modified Cahn-Hilliard equation is used. In that way the capillary force  $F_c$  responsible for the wrapping is directly resolved. The already existing model will be extended to describe the interaction using anisotropic contact angle. At the initial phase of WP 1.5 a two week visit of a PhD student (P2) of the IOM (requested in this proposal) at the HZDR is planned. The aim of the visit is the consolidation of the cooperation of the IOM and the HZDR as well as the qualification of the PhD student to perform the simulation. The simulation will be compared with the results from WP 1.4 and the physical description will be potential adopted and extended. The optimized model will be used to optimize the necessary surface and substrate properties.

Consequently the WP 1.5 is separated in sub-packages:

- (a) Create the physical description and generate the simulation supported by HZDR
- (b) Comparison of the experimental results with simulation and adaption as well as extension of the physical description
- (c) Using the optimized simulation to optimized the surface and bulk properties of the polymere film

## Phase II: Production of self-folding 3D structures

Based on the results of Phase I, the aim of Phase II is to produce the self-folding 3D structures. For this purpose, the findings of Phase I are used to detect suitable substrate and surface modifications and to adapt them if necessary (WP 2.1). The planned plane structures for the 3D basic structures produced from prepared samples by laser (WP 2.2) and lithography (WP 2.3). The self-folding process is time-resolved recorded by a measuring system that is constructed in WP 2.4. The results compared with the simulated behavior (WP 2.5.). Based on the results of WP 2.4 and WP 2.5, the substrate and surface modifications (WP 2.1), as well as the sample geometries (WP 2.2 and 2.4), are adjusted and optimized. The aim is to evaluate the possibilities and limitations of self-folding processes using anisotropic substrate properties and anisotropic contact angles.

### Work package WP 2.1 Optimization and adaptation of surface and substrate modification

The first step in WP 2.1, suitable substrate and surface modifications are the selection for use in the self-folding process. The selection criteria are i.e., long-time stability, variation of the contact angle. The specific selection criteria derived from the results of Phase I.

In the second step in WP 2.2, the substrate and surface modifications are specifically adapted and optimized, based on the findings of Phase I and in particular on the predictions from the simulation of L-S-I and the induced bending.

### Work package WP 2.2 Laser structuring of flexible substrates for 3D structures

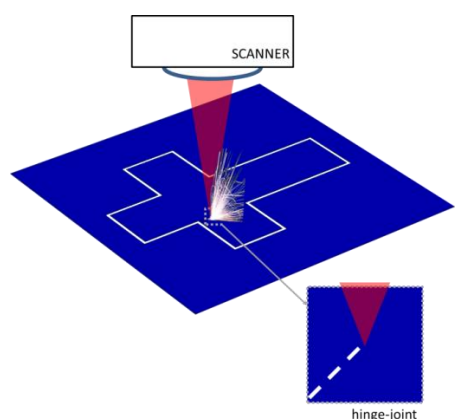


Figure 14: Schematic illustration of the laser-assisted structuring process

The selected samples with suitable substrate and surface modifications patterned by pulsed laser radiation. The generated plan basic structures used for 3D self-folding processes (see Fig. 14). The laser-assisted structuring allows a fast, flexible, and direct production of structured samples. For the laser-assisted production of high-precision extruded geometries with "hinge joints" (hinge joints: reduction of the layer thickness and / or partial perforation of the flexible substrate at the fold edges to support the folding process) from planar substrates (see Fig. 14), an optimization of the laser process is necessary. The optimization carried out under the following objective: High-dimensional accuracy of the geometry of the released samples, high edge accuracy, and low thermal modification of the sample edges. To achieve the objective, an adaptation

of the laser parameters and the laser beam scan procedure is necessary.

### Work package WP 2.3 "Classic" structuring of flexible substrates for 3D structures

In addition to the laser structuring, a structuring by lithography provided. In contrast, the lithographic technologies allow simple mass production of structures in comparison to laser structuring. The optimized lithographic process allows an easy transfer of the experimental results into an industrial application considering the results in a follow-up project. The manufacturing process is shown schematically illustrated in Figure 15. The application and the photolithographic development of the photoresist as well as the wet-chemical treatment of the photoresist is a well-established technology, which also carried out in the IOM for many years. Within the framework, no further optimization of the process is to be expected. However, the defined structuring of the flexible substrate requires a specific adaptation. The objective is in accordance with WP 2.2: high form accuracy and high edge accuracy with low edge modifications. Successful structuring requires a selective physical structuring process. To achieve this, a multi-level structuring process is necessary (see Fig. 15).

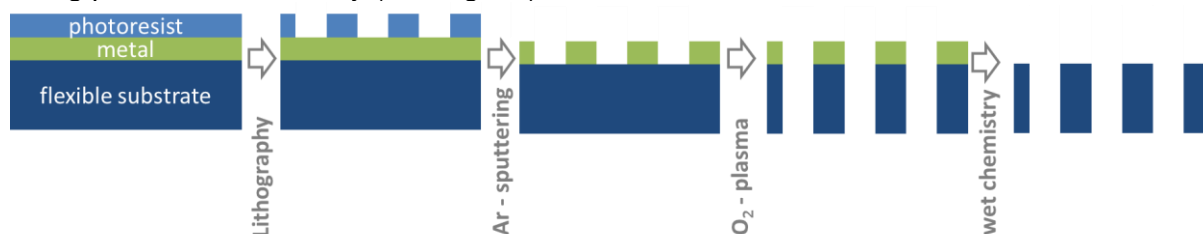


Figure 15: Schematic illustration of the structuring process

The flexible substrate is coated with metal and subsequently covered with photoresist. The photolithographic treatment result in a structuring of the photoresist and the subsequent argon sputtering leads to the structuring of the metal. The oxygen plasma treatment of the structured metal layer allows a structuring of the flexible substrate up to complete perforation. The concept of the envisaged process was already successfully tested for the production of structures with high aspect ratios [E5].

### Work package WP 2.4 Generation and characterization of the 3D folding process

In order to characterize the produced structures (WP 2.1 - 2.3), the measurement of the 3D folding process is necessary. For this purpose, the optical setup constructed in WP 1.3 is used for the time-resolved measurement of the folding process. The folding process is created by applying a liquid drop such as H<sub>2</sub>O with a defined volume, whereby the L-S-I leads to a folding process (see Fig. 16).

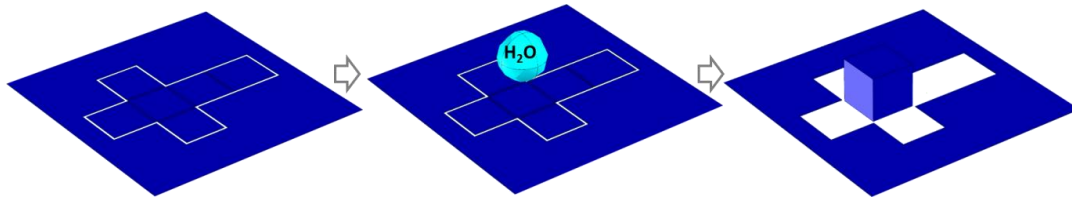


Figure 16: Schematic illustration of the liquid drop induced 3D self-folding process

Within WP2.4, two different liquid droplet feeds are tested:

- Directly sprinkling the front side of the structured flexible substrate by means of a micropipette
- Supplying the liquid from the back of the structured flexible substrate, for which purpose the flexible substrate is locally perforated

The dynamic folding process measured depending on the surface and substrate modifications (WP 2.1) as well as on the sample geometry (WP 2.2 and 2.3). Based on the results, the parameters (WP 2.1 - 2.3) was optimized.

### Work package WP 2.5 Simulation of the 3D folding process (supported by HZDR)

Based on the results of WP 1.5, work package WP 2.5 simulates the 3D folding process as a function of the surface and substrate modifications as well as the sample geometry. The initialization of the WP 2.5 start with a second visit of a PhD student (P2) from the IOM (requested at this proposal)

The WP 2.5 can be divided into the following subtasks:

- (a) Simulation of the dynamic self-folding process.
  - Adaptation of the physical description and simulation developed in WP 1.5
  - Description of the 3D self-folding process measured in WP 2.4
- (b) Optimization of surface / substrate modification and sample geometry
  - The successful physical description and simulation of the folding process is used for the simulation-based optimization of the surface / substrate modification and sample geometry, including the hinge geometry.
- (c) Estimation of the limits of the self-folding process
  - The simulation will continue to use to estimate the possibilities of the self-convolution process.

The temporal sequence of the individual works summarized in the following bar chart:



Table 1: Schematic representation of the timetable (color-coded: blue performed by IOM, red: supported by HZDR; P1: WP performed by PhD student 1, P2: WP performed by PhD student 2).

	first year				second year				third year			
	1. Q	2. Q	3. Q	4.Q	1. Q	2. Q	3. Q	4.Q	1. Q.	2. Q	3. Q	4.Q
WP1.1	P1	P1										
WP1.2			P1	P1								
WP1.3					P1	P1						
WP1.4	P1/P2	P1/P2		P1/P2		P1/P2						
WP1.5	P2	P2	P2	P2	P2	P2						
WP2.1							P1	P1			P1	
WP2.2								P1	P1	P1		
WP2.3											P1	P2
WP2.4								P1/P2				P1/P2
WP2.5							P2	P2	P2	P2	P2	P2
	PHASE 1						PHASE 2					

## Data handling

The collected data are stored in primary form. This first locally occurs on the different computers. Regularly, the data merged into a special project folder, thematically ordered on a secure drive. The derived data such as graphs, films, reports, etc. also archived there. The research data used in particular for scientific publications and to evaluate the economic recoverability through presentations at workshops, conferences and technical reports.

## 3 Bibliography

- [1] T. Young, Phil. Trans. R. Soc. Lond. 95 (1805) 65.
- [2] F. M. Ma et al., Mater. Res. Express 4 (2017) 092001
- [3] R. N. Wenzel, Ind. Eng. Chem. 28, (1936) 988.
- [4] A. B. D Cassie et al., Trans. Faraday Soc. 40 (1944) 546.
- [5] A. Bussonniere et al., Soft Matter 13 (2017) 978.
- [6] C Extrand, Langmuir. 18 (2002) 7991.
- [7] L. He et al, Colloids and Surfaces A 553 (2018) 67.
- [8] Y. C. Lee et al., Sensors and Actuators a-Physical 93 (2001) 57.
- [9] E. C. Harvey et al., Proc. of SPIE 2639 (1995) 266.
- [10] K. Zimmer et al., Applied Surface Science 96-8 (1996) 425.
- [11] K. Zimmer et al.,Proc. of SPIE 4236 (2001) 58.
- [12] A. Braun et al., Applied Surface Science 186 (2002) 200.
- [13] K. Zimmer et al., Excimer laser machining for 3D-surface structuring, In: Photo-Excited Processes, Diagnostics and Applications, Ed. A. Peled, Kluwer, Boston (2003).
- [14] K. Zimmer et al., Applied Surface Science 154 (2000) 601.
- [15] K. I. Jolic et al., Journal of Micromechanics and Microengineering 14 (2004) 388.
- [16] C. C. Chiu et al., Opt. Lasers Eng. 49 (2011) 1232.
- [17] A. S. Holmes et al., Proc. SPIE Photonics West, 5713 (2005) 180.
- [18] N.A.M Araújo et al., Physical Review Letters 120 (2018) 188001.
- [19] R. J. Lang et al., Applied Mechanics Reviews 70 (2018) 010805.
- [20] K. Kuribayashi-Shigetomi et al., PLOS ONE 7 (2012) e51085.
- [21] K. Malachowski et al., Nano Lett. 14 (2014) 4164.
- [22] S. Miyashita et al., Smart Mater. Struct. 23 (2014) 094005
- [23] N. Goshi et al., J. Micromech. Microeng. 28 (2018) 065009
- [24] C. Py et al., PRL 98 (2007) 156103.
- [25] A. Legrain et al., Journal of Applied Physics 115 (2014) 214905.
- [26] C. Py et al., Eur. Phys. J. Special Topics 166 (2009) 67.
- [27] K. Kobayashi et al., Macromol. Rapid Commun. 39 (2018) 1700692.
- [28] M. Pineirua et al., Soft Matter 6 (2010) 4491.
- [29] S. Tawfick et al., Adv. Mater. 24 (2012) 1628.
- [30] P. Lorenz et al., Physics Procedia 83 (2016) 62.
- [31] G. Lecrivain et al., Physical Review Fluids, 2018.

#### 4 Requested modules/funds

##### 4.1 Basic Module

##### 4.1.1 Funding for Staff

1	N.N. PhD student 1 (P1) (TV-L EG 13, 75 %; 3 years, employed by IOM)	from total funds	10/19 145 T€
	<u>Task:</u> Performing experiments, implementation and monitoring of the analysis of the structures, evaluation and systematization of experiments, interpretation on the basis of physical relationships where the individual task are: - Surface and bulk modification of flexible polymer films - Characterization of the produced modifications - Construction and commissioning of measurement system for dynamic measurement of the contact angle and the self-folding process as well as the L-S-I induced forces in cooperation with PhD student 2 (P2) - Performing of systematic measurements on the build measurement system in cooperation with P2 - Structuring of modified polymer films for self-folding processes		
2	N.N. PhD student 2 (TV-L EG 13, 75 %; 3 years, employed by IOM)		10/19 145 T€
	<u>Tasks:</u> Simulation of the L-S-I and the self-folding process and performing of experiments where the individual task are: - Construction and commissioning of measurement system for dynamic measurement of the contact angle and the self-folding process as well as the L-S-I induced forces in cooperation with P1 - Performing of systematic measurements on the build measurement system in cooperation with P1 - Physical description and simulation of the L-S-I and the self-folding process - Based on the experimental result adaption of the physical description and improving of the simulation		
3	Student/graduate assistants 19 hours/month for 2 years, € 8.56/hr.	from total funds	10/19 17 T€
	<u>Task:</u> Routine experimentation, data collection and evaluation		

##### 4.1.2 Direct Project Costs

Devices, software, consumables		
Laboratory consumables, samples, sputtering targets for sample preparation		7 T€
Analytic consumption (AFM, SIMS, SEM)		5 T€
Electronic materials for experimental set-ups		5 T€
Optical elements		9 T€
	Σ	26 T€

##### 4.1.2.1 Travel Expenses

Travel funds		
An annual visit to a scientific meeting in Europe (e.g. EMRS, GAMM) for 1 person		6 T€
An annual visit of an academic conference outside Europe (e.g. COLA, SPIE Photonic West) for 1 person		6 T€
PhD student visit of HZDR (10 days + 5 days)		400 €
SPP events		2 T€
	Σ	14.4 T€

#### 4.1.2.2 Project-related publication expenses

Publication costs

2 T€

### 5 Project requirements

#### 5.1 Employment status information

Pierre Lorenz, research scientist, temporary appointment (employed till 12/18, funded by DFG ZI 660/13-2, a further appointment is scheduled.)

#### 5.2 First-time proposal data

*Only if applicable: Last name, first name of first-time applicant*

#### 5.3 Composition of the project group

Dr.	Pierre Lorenz	scientist	temporary appointment
Dr.-Ing.	Klaus Zimmer	group leader	permanent appointment
Dr.	Joachim Zajadacz	scientist	temporary appointment
Dr.	Martin Ehrhardt	scientist	temporary appointment
	N.N.	PhD student 1	requested here
	N.N.	PhD student 2	requested here
	N.N.	student assistant	requested here

#### 5.4 Cooperation with other researchers

##### 5.4.1 Researchers with whom you have agreed to cooperate on this project

Gregory Lecrivain, Dr. rer. nat.  
Helmholtz-Zentrum Dresden-Rossendorf  
Institut für Fluidodynamik  
Bautzner Landstraße 400, 01328 Dresden  
Phone: +49 351 260 – 3768  
E-mail: g.lecrivain@hzdr.de

##### 5.4.2 Researchers with whom you have collaborated scientifically within the past three years

Andreas Otto, Prof Dr.-Ing. Dipl. Phys.  
Institute of Production Engineering and Laser Technology (Institut für Fertigungstechnik und Hochleistungslasertechnik), TU Wien  
Phone: +43 (1) 58801 - 311 622 E-Mail: andreas.otto@tuwien.ac.at  
Getreidemarkt 9 1060 Wien

Patrick Schwaller, Prof. Dr. and Beat Neuenschwander, Prof. Dr.  
Institute for Applied Laser, Photonics and Surface Technologies ALPS  
Bern University of Applied Science - Engineering and Information Technology  
Pestalozzistr. 20, CH-3400 Burgdorf

#### 5.5 Scientific equipment

The following systems will be most likely used for the project. At the IOM a variety of devices are also available.

Thin film fabrication and structuring:

- Clean rooms and equipment for the processing of surfaces and thin films for micro-/nanostructuring,
- Sputtering and evaporation systems for metals and dielectrics,
- Photolithography for 6" incl. wet-chemical methods for pattern transfer,
- Electron beam lithography for 4" with 2 axis laser Interferometer table
- Reactive ion beam etching (RIE)

Laser systems: Laser material processing systems including spot movement, camera system, focusing optics, CNC (wavelength; pulse duration, spot size; repetition; sample size; power):

- Excimer laser: 353, 248, 193 nm;  $\sim 20$  ns;  $(2\text{ }\mu\text{m})^2$  to  $(2\text{ mm})^2$ ; to 100 Hz;  $(200\text{ mm})^2$ ; max. 40 W,
- Pyrophotonics Pyroflex 25-IR (1064 nm, pulse widths free of 1–600 ns programmable, repetition 2–500 kHz, average power 25 W, pulse energy 0–0.6 mJ),
- 1.5  $\mu\text{m}$  laser (Manlight MLT-PL-R-OEM 65-05-100-1000;  $\lambda = 1550$  nm,  $P = 10$  W,  $E_{\text{puls}} = 100\text{ }\mu\text{J}$ ,  $\Delta t_p \sim 5$  ns,  $f = 100$  kHz to 300 kHz),
- Nd:YVO<sub>4</sub> ps-laser ( $\lambda_0 = 1064$  nm,  $\lambda_1 = 532$  nm,  $\lambda_3 = 355$  nm,  $\Delta t_p = 12$  ps,  $f \leq 500$  kHz),
- Ti:Al<sub>2</sub>O<sub>3</sub> fs-laser ( $\lambda_0 = 1064$  nm,  $f = 1$  kHz,  $\Delta t_p = 150$  fs).

Analytical systems:

- Scanning electron microscopy (SEM) with energy-dispersive X-ray spectroscopy (EDX) and electron backscatter diffraction (EBSD),
- Crossed beam workstation (focused ion beam - FIB) for the production of site-specific micro cross sections (e.g. for TEM lamellae preparation or SEM illustration),
- Photoelectron spectroscopy (XPS),
- Time-of-flight secondary ion mass spectrometry (TOF-SIMS),
- Transmission electron microscopy (TEM) inclusive sample preparation,
- Atomic force microscopy (AFM) and scanning electron microscopy (STM) (digital instruments) with different probes and methods of measurement,
- White light interferometry (WLI) for measuring topography,
- Profilometer for determining layer thickness,
- High-temperature ellipsometer Woolam M2000 ellipsometer,
- Thin film metrology spectroscopic reflectometer with mapping function up to 400 mm,
- A variety of electrical and optical measurements.

The mentioned devices are utilized by other ongoing projects.

## 6 Additional information

An application for funding of this project not submitted to another sponsor. If such a request submitted, the DFG will notified immediately. The Institute Director of the IOM is informed. The rules of good scientific practice are recognized.

The IOM supports family friendliness word. Since 2011, the institute hold an "audit berufundfamilie" certificate.